International Journal of Mathematical Archive-6(9), 2015, 164-177
Available online through www.ijma.info ISSN 2229 – 5046

GALERKIN FINITE ELEMENT SOLUTION OF MHD FREE CONVECTION RADIATIVE FLOW PAST AN INFINITE VERTICAL POROUS PLATE WITH CHEMICAL REACTION AND HALL CURRENT

J. ANAND RAO[1], P. RAMESH BABU*[2], R. SRINIVASA RAJU

[1]Department of Mathematics, University College of Science,
Osmania University, Hyderabad, 500007, Andhra Pradesh, India.

[2]Department of Mathematics, Guru Nanak Institute of Technology, Khanapur(vil),
Ibrahimpatnam, Ranga Reddy (Dt), 501506, Hyderabad, Telangana State, India.

*Department of Mathematics, GITAM University,
Hyderabad Campus, Rudraram, Medak (Dt), 502329, Telangana State, India.

(Received On: 02-09-15; Revised & Accepted On: 28-09-15)

ABSTRACT

Chemical reaction and radiation effects on an unsteady free convection flow of an electrically conducting gray gas near equilibrium in the optically thin limit along an infinite vertical porous plate are investigated in the presence of strong transverse magnetic field imposed perpendicularly to the plate, taking hall currents in to account. The similarly equations were obtained using suitable transformations and the resulting non – linear coupled partial differential equations are solved by Galerkin finite element method. A parametric study illustrating the influence of different flow parameters on velocity, temperature and concentration fields are investigated. The skin – frictions at the plate due to the primary and secondary velocity fields and the rate of heat and mass transfer co – efficient are obtained in non – dimensional form. The effects of different flow parameters on these respective fields are discussed through graphs and tables and results are physically interpreted.

Keywords: *Thermal Radiation, Chemical reaction, Hall current, MHD, Galerkin Finite element method.*

NOMENCLATURE

h	Length scale of similarity parameter
q_r	Radiant heat transfer
C'	Dimensional Species Concentration
C'_w	Wall dimensional Concentration
C'_∞	Species concentration at infinity
I	Current across the plate length
$e_{b\lambda}$	Plank's function
T'	Temperature of a fluid
T'_∞	Fluid temperature at infinity
T'_w	Wall dimensional temperature
$k_{\lambda\omega}$	Mean absorption coefficient
(x', y', z')	Cartesian coordinates
B_o	Strength of applied Magnetic field
$\overline{K}$	Chemical reaction of first order with rate constant
t'	Time
v_0	Non – dimensional transpiration parameter
$v_0 > 0$	Suction
$v_0 < 0$	Injection
g	Acceleration due to gravity
v'	Velocity component in $y'-$ direction
G'	Velocity component in $z'-$ direction
F'	Velocity component in $x'-$ direction
u	Non – dimensional velocity
C	Non – dimensional concentration
k	Thermal conductivity
C_p	Specific heat of the fluid at constant pressure
D	Chemical molecular diffusivity
Kr	Dimensional chemical reaction parameter
u_0	Free stream velocity
Gr	Grashof number
Gc	Modified Grashof number
m	Hall parameter

Corresponding Author: P. Ramesh Babu*[2]

M	Hartmann number
Pr	Prandtl number
R	Radiation parameter
Nu	Nusselt number (or) heat transfer coefficient
Sh	Sherwood number (or) mass transfer coefficient
Sc	Schmidt number
k_r	Non – dimensional Chemical reaction parameter
a_0	Half of non – dimensional transpiration parameter

Greek symbols:

θ	Non – dimensional temperature
β	Volumetric coefficient of Thermal expansion
β^*	Volumetric coefficient of expansion with concentration
μ_e	Magnetic permeability of the medium
σ	Electrical conductivity
ρ	Fluid density
τ_1	Skin – friction at the wall along $x' -$ axis
τ_2	Skin – friction at the wall along $z' -$ axis
η	Dimensionless coordinate
ω	Frequency of oscillation
λ	Non – dimensional transpiration cooling parameter

1. INTRODUCTION

The present trend in the field of chemical reaction analysis is to give a mathematical model for the system to predict the reactor performance. A large amount of research work has been reported in this field. In particular, the study of heat and mass transfer with chemical reaction is of considerable importance in chemical and hydrometallurgical industries. Chemical reaction can be codified as either heterogeneous or homogeneous processes. This depends on whether they occur at an interface or as a single phase volume reaction. Frequently the transformations proceed in a moving fluid, a situation encountered in a number of technological fields. A common area of interest in the field of aerodynamics is the analysis of thermal boundary layer problems for two – dimensional steady and incompressible laminar flow passing a wedge. Simultaneous heat and mass transfer from different geometrics embedded in a porous media has many engineering and geophysical applications such as geothermal reservoirs, drying of porous solids, thermal insulation, enhanced oil recovery, packed – bed catalytic reactors, cooling of nuclear reactors and underground energy transport. A very significant area of research in radiative heat transfer, at the present time is the numerical simulation of combined radiation and convection or conduction transport processes. The effort has arisen largely due to the need to optimize industrial system such as furnaces, ovens and boilers and the interest in our environment and in non conventional energy sources, such as the use of salt – gradient solar ponds for energy collection and storage. In particular, natural convection induced by the simultaneous action of buoyancy forces resulting from thermal and mass diffusion is of considerable interest in nature and in many industrial applications such as geophysics, oceanography, drying processes, solidification of binary alloy and chemical engineering. Frequently the transformations proceed in a moving fluid, a situation en – countered in a number of technological fields. The effect of chemical reaction on an unsteady magnetohydrodynamic free convection flow past a semi – infinite vertical plate embedded in a porous medium with heat absorption by applying finite element method discussed by Anand Rao *et al.* [1]. The effects of heat and mass transfers on an unsteady magnetohydrodynamic flow past a vertical plate under oscillatory suction velocity by applying finite element method studied by Anand Rao *et al.* [2]. The effect of hall current on an unsteady magnetohydrodynamic transient flow past an impulsively started infinite horizontal porous plate in a rotating fluid by applying finite element method studied by Anand Rao *et al.* [3]. Chamka and Ahmed [6] found the similarity solution for an unsteady magnetohydrodynamic flow near a stagnation point of a three – dimensional porous body with heat and mass transfer, heat generation/absorption and chemical reaction. Finite difference solution of the homogeneous first order chemical reaction on unsteady flow past an impulsively started semi – infinite vertical plate with variable temperature and mass diffusion in the presence of thermal radiation have been studied by Loganathan *et al.* [12]. The fluid considered here is a gray, absorbing – emitting radiation but a non – scattering medium. The dimensionless governing equations are solved by an efficient, more accurate, unconditionally stable and fast converging implicit scheme. Mansour *et al.* [13] investigates the influence of chemical reaction and viscous dissipation on magnetohydrodynamic natural convection flow. An approximate numerical solution for the flow problem has been obtained by solving the governing equations using shooting technique with a fourth – order Runge – Kutta integration scheme. Four different cases of flows have been studied namely an isothermal surface, a uniform heat flux surface, a plane plume and flow generated from a horizontal line energy source a vertical adiabatic surface. The effects of temperature dependent heat source on the free convection and mass transfer flow past an exponentially accelerated infinite vertical plate of a viscous incompressible electrically conducting fluid under the action of a uniform magnetic field through porous medium studied by Rajesh and Varma [16]. The dimensionless governing equations are solved in closed form by the Laplace transform technique. Greif *et al.* [9] showed that, for an optically thin limit, the fluid does not absorb its own emitted radiation, this means that there is no self absorption, but the fluid does absorb radiation emitted by the boundaries. In space technology and in nuclear engineering applications, such a problem is quite common. But in these fields, the presence of strong magnetic field and hall current taking effects play an important role and these effects have not been studied in the case of free convective flow of radiation gas under the condition

mentioned above. Seth *et al.* [20] discussed the effect of hall current and rotation on an unsteady magnetohydrodynamic Couette flow in the presence of an inclined magnetic field by applying Laplace transform technique. However, Cogley *et al.* [7] showed that, in the optically thin limit for a gray gas near equilibrium the following relation holds:

$$\frac{\partial q_r}{\partial y'} = 4\left(T' - T_w'\right)I \tag{1}$$

Where $I = \int_0^\infty k_{\lambda\omega}\left(\frac{\partial e_{b\lambda}}{\partial T'}\right)_\omega d\lambda$ (2)

In all these studies, the effect of radiation is not considered. In space technology applications and at higher operating temperatures, radiation effects can be quite significant. Since radiation is quite complicated, many aspects of its effect on free convection or combined convection have not been studied in recent years. Radiation and mass transfer effects on an unsteady magnetohydrodynamic convective and dissipative fluid flow past a vertical porous plate has been analyzed by Gnaneswara Reddy and Bhaskar Reddy [8]. The governing equations of motion, energy and species are transformed into ordinary differential equations using time dependent similarity parameter. The numerical study of thermal radiation effects on the transient hydromagnetic natural convection flow past a vertical plate embedded in a porous medium with mass diffusion and fluctuating temperature about time at the plate, by taking into account the heat due to viscous dissipation studied by Kishore *et al.* [11]. The governing equations are solved by an implicit finite difference method of Crank – Nicolson type. Influence of thermal radiation on transient magnetohydrodynamic Couette flow through a porous medium by using finite difference method discussed by Baoku *et al.* [5]. Raji Reddy and Srihari [17] studied numerical solution of unsteady flow of a radiating and chemically reacting fluid with time – dependent suction. The effects of radiation on a steady combined free – forced convective and mass transfer flow of a viscous incompressible electrically conducting and radiating fluid over an isothermal semi – infinite vertical porous flat plate embedded in a porous medium studied by Bala Anki Reddy and Bhaskar Reddy [4]. The governing non – linear partial differential equations and their boundary conditions are reduced into a system of ordinary differential equations by a similarity transformation. This system is solved numerically using Runge – Kutta fourth order method along with shooting technique. Sankar Reddy *et al.* [18] studied the effect of thermal radiation on unsteady two – dimensional laminar flow of a viscous incompressible electrically conducting micropolar fluid past a semi – infinite vertical porous moving plate taking into account the effect of magnetic field in the presence of heat absorption. The Rosseland approximation is used to describe radiative heat transfer in the limit of optically thick fluids. The dimensionless governing equations for this investigation are solved analytically using perturbation technique. Analytical solutions for heat and mass transfer by laminar flow of a Newtonian, viscous, electrically conducting and heat generation/absorbing fluid on a continuously vertical permeable surface in the presence of a radiation, a first – order homogeneous chemical reaction and the mass flux are reported by Kesavaiah *et al.* [10]. The plate is assumed to move with a constant velocity in the direction of fluid flow. A uniform magnetic field acts perpendicular to the porous surface, which absorbs the fluid with a suction velocity varying with time. The dimensionless governing equations for this investigation are solved analytically using two – term harmonic and non – harmonic functions. Mohammed Ibrahim and Bhaskar Reddy [14] analyzed the radiation effects on the heat and mass transfer characteristics of a viscous incompressible electrically conducting fluid near an isothermal vertical stretching sheet, in the presence of viscous dissipation and heat generation. The governing equations are transformed by using similarity transformation and the resultant dimensionless equations are solved numerically using the Runge – Kutta fourth order method with shooting technique. Mohammed Seddeek and Aboeldahab [22] studied the effect of radiation on an unsteady free convection flow of an electrically conducting, gray gas near equilibrium in the optically thin limit along an infinite vertical porous plate are investigated in the presence of strong transverse magnetic field imposed perpendicularly to the plate, taking hall currents into account. The effect of radiation on unsteady free convection flow past a semi – infinite vertical porous plate embedded in a porous medium with heat and mass transfer in the presence of transverse uniform magnetic field with blowing and suction has been analyzed by Prasad *et al.* [15]. The governing boundary layer equations for this problem are transformed in to a linear algebraic system under solved numerically by an implicit finite difference method. Vasu *et al.* [21] studied the radiation and mass transfer effects on transient free convection flow of a dissipative fluid past semi – infinite vertical plate with uniform heat and mass flux.

The objective of the present paper is to analyze the radiation and chemical reaction effects on an unsteady magnetohydrodynamic free convection fluid flow past an infinite vertical porous plate with hall current. The dimensional less equations of continuity, linear momentum, energy and diffusion, which govern the flow field, are solved numerically by using an efficient finite element method which is more economical from computational view point and the results obtained are good agreement with the results of Mohammed Seddeek and Aboeldahab [22] in some special cases. The behavior of the velocity, temperature, concentration, skin – friction coefficient, Nusselt number and Sherwood number has been discussed for variations in the governing parameters.

2. MATHEMATICAL FORMULATION

Consider an unsteady free convection flow of a viscous incompressible and electrically conducting fluid along an infinite vertical porous plate subjected to time – dependent suction velocity. We made the following assumptions:

1. The $x'-$axis is taken to be along the plate and $y'-$axis normal to the plate. Since the plate is considered infinite in $x'-$direction, hence all physical quantities will be independent of $x'-$direction. Therefore, all the physical variables become functions of y' and t' only.
2. The wall is maintained at constant temperature T_w' and concentration C_w' higher than the ambient temperature T_∞' and concentration C_∞' respectively.
3. The viscous dissipation and the joule heating effects are negligible in the energy equation.
4. The homogeneous chemical reaction of first order with rate constant $\overline{K}$ between the diffusing species and the fluid is assumed.
5. A uniform magnetic field of magnitude B_o is applied normal to the plate. The transverse applied magnetic field and magnetic Reynolds number are assumed to be very small, so that the induced magnetic field is negligible.
6. Electric field is neglected.
7. The concentration of the diffusing species in the binary mixture is assumed to be very small in comparison with the other chemical species, which are present and hence the Soret and Dufour effects are negligible.

Under the above assumptions as well as Boussinesq's approximation, the equations of conservation of mass, momentum, energy and concentration governing the free convection boundary layer flow over a vertical porous plate can be expressed as:

Equation of Continuity:

$$\frac{\partial v'}{\partial y'}=0 \tag{3}$$

Momentum Equation:

$$\frac{\partial F'}{\partial t'}+v'\frac{\partial F'}{\partial y'}=g\beta\left(T'-T_\infty'\right)+g\beta^*\left(C'-C_\infty'\right)+v'\frac{\partial^2 F'}{\partial y'^2}-\frac{\sigma\mu_e^2 B_o^2}{\rho\left(1+m^2\right)}\left(F'+mG'\right) \tag{4}$$

$$\frac{\partial G'}{\partial t'}+v'\frac{\partial G'}{\partial y'}=\frac{\partial^2 G'}{\partial y'^2}+\frac{\sigma\mu_e^2 B_o^2}{\rho\left(1+m^2\right)}\left(mF'-G'\right) \tag{5}$$

Energy Equation:

$$\frac{\partial T'}{\partial t'}+v'\frac{\partial T'}{\partial y'}=\frac{k}{\rho C_p}\frac{\partial^2 T'}{\partial y'^2}-\frac{4\left(T'-T_w'\right)}{\rho C_p}I \tag{6}$$

Species Diffusion Equation:

$$\frac{\partial C'}{\partial t'}+v'\frac{\partial C'}{\partial y'}=D\frac{\partial^2 C'}{\partial y'^2}-K_r\left(C'-C_\infty'\right) \tag{7}$$

And the corresponding boundary conditions are given by

$$\begin{Bmatrix} t'\le 0:\left\{F'=0,\ \ G'=0,\ \ T'=0,\ \ C'=0 \quad for\ all\ y'\right\} \\ t'>0:\begin{cases} F'=0,\ \ G'=0,\ \ T'=T_w',\ \ C'=C_w' & at\ y'=0 \\ F'\to 0,\ G'\to 0,\ T'\to T_\infty',\ C'\to C_\infty' & at\ y'\to 0 \end{cases} \end{Bmatrix} \tag{8}$$

We now define the similarity variables as follows:

$$F'=u_o u(\eta),\ \ G'=u_o w(\eta),\ \ \theta(\eta)=\frac{\left(T'-T_\infty'\right)}{\left(T_w'-T_\infty'\right)},\ \ \phi(\eta)=\frac{\left(C'-C_\infty'\right)}{\left(C_w'-C_\infty'\right)},\ \ \eta=\frac{y'}{h} \tag{9}$$

Where $h\left(=h(t)\right)$ is a similarly parameter length scale and u_0 is the free stream velocity. In terms of $h(t)$, a convenient solution of (3) can be given by

$$v' = -v_o\left(\frac{u}{h}\right) \tag{10}$$

Where v_0 is a non – dimensional transpiration parameter, clearly $v_0 > 0$ and $v_0 < 0$ indicates suction or injection respectively.

Accordingly (4), (5), (6) and (7) take the form

$$-\frac{h}{v'}\frac{\partial h}{\partial t'}\eta u' - v_o F' = F'' - (Gr)\theta + (Gc)\phi + \frac{M}{\left(1+m^2\right)}\left(u + mw\right) \tag{11}$$

$$-\frac{h}{v'}\frac{\partial h}{\partial t'}\eta G' - v_o G' = G'' - \frac{M}{\left(1+m^2\right)}\left(mu - w\right) \tag{12}$$

$$-\frac{h}{v'}\frac{\partial h}{\partial t'}\eta\theta' - v_o\theta' = \frac{1}{\Pr}\theta'' - R\left(\theta - 1\right) \tag{13}$$

$$-\frac{h}{v'}\frac{\partial h}{\partial t'}\eta\phi' - v_o\phi' = \frac{1}{Sc}\phi'' - k_r\phi \tag{14}$$

Where $Gr = g\beta h^2\,\frac{\left(T_w' - T_\infty'\right)}{v'^2}$, $\Pr = \frac{\rho v' C_p}{k}$, $Gc = g\beta^* h^2\,\frac{\left(C_w' - C_\infty'\right)}{v'^2}$, $M = \frac{\sigma\mu_e^2 B_o^2 h^2}{v'\rho}$, $Sc = \frac{v'}{D}$,

$R = \frac{4Ih^2}{\rho C_p v'}$, $k_r = \frac{K_r}{v'^2}$

The boundary conditions corresponding to the equations (11), (12), (13) and (14) are

$$\left.\begin{array}{ll} u = 0, \quad w = 0, \quad \theta = 1, \quad \phi = 1 & at\ \eta = 0 \\ u \to 0,\ w \to 0,\ \theta \to 0,\ \phi \to 0 & as\ \eta \to \infty \end{array}\right\} \tag{15}$$

Equations (11), (12), (13) and (14) are similar except for the term $\left(\frac{h}{v'}\right)\left(\frac{\partial h}{\partial t'}\right)$ where t' appears explicitly. Thus, the similar condition requires that $\left(\frac{h}{v'}\right)\left(\frac{\partial h}{\partial t'}\right)$ must be constant.

Hence it is assumed that $\left(\frac{h}{v'}\right)\left(\frac{\partial h}{\partial t'}\right) = C_1$ (16)

Where C_1 is an arbitrary constant.

At C_1 = 2 and by integrating equation (16), one obtain $h = 2\sqrt{v't'}$ which defines the well – established scaling parameter for unsteady boundary layer problems Schlichting [19]. Hence, the similarity equations are obtained as

$$u'' + 2\left(\eta + a_o\right)u' = -(Gr)\theta - (Gc)\phi + \frac{M}{\left(1+m^2\right)}\left(u + mw\right) \tag{17}$$

$$w'' + 2\left(\eta + a_o\right)w' = \frac{M}{\left(1+m^2\right)}\left(mu - w\right) \tag{18}$$

$$\theta'' + 2(\Pr)\left(\eta + a_o\right)\theta' - \left(R\right)(\Pr)(\theta - 1) = 0 \tag{19}$$

$$\phi'' + 2\left(Sc\right)\left(\eta + a_o\right)\phi' - \left(k_r\right)(Sc)\phi = 0 \tag{20}$$

Where $a_o = \frac{v_o}{2}$

The skin – friction, Nusselt number and Sherwood number are important physical parameters for this type of boundary layer flow. The skin – friction at the plate, which in the non – dimensional form is given by

$$\tau_1 = -\left(\frac{\partial u}{\partial \eta}\right)_{\eta=0} \quad \& \quad \tau_2 = -\left(\frac{\partial w}{\partial \eta}\right)_{\eta=0} \tag{21}$$

The rate of heat transfer coefficient, which in the non – dimensional form in terms of the Nusselt number is given by

$$Nu = -\left(\frac{\partial \theta}{\partial \eta}\right)_{\eta=0} \tag{22}$$

The rate of mass transfer coefficient, which in the non – dimensional form in terms of the Sherwood number, is given by

$$Sh = -\left(\frac{\partial \phi}{\partial \eta}\right)_{\eta=0} \tag{23}$$

3. METHOD OF SOLUTION

By applying Galerkin finite element method for equation (17) over the element (e), $(\eta_j \le \eta \le \eta_k)$ is:

$$\int_{\eta_j}^{\eta_k} N^T \left\{\frac{\partial^2 u^{(e)}}{\partial \eta^2} + A\frac{\partial u^{(e)}}{\partial \eta} - Bu^{(e)} - P\right\} d\eta = 0 \tag{24}$$

Where $A = 2(\eta + a_o)$, $B = \frac{M}{1+m^2}$, $P = -(Gr)\theta - (Gc)\phi + Bmw$;

Integrating the first term in equation (24) by parts one obtains

$$N^{(e)T}\left\{\frac{\partial u^{(e)}}{\partial \eta}\right\}_{\eta_j}^{\eta_k} - \int_{\eta_j}^{\eta_k}\left\{\frac{\partial N^{(e)T}}{\partial \eta}\frac{\partial u^{(e)}}{\partial \eta} + N^{(e)T}\left(A\frac{\partial u^{(e)}}{\partial \eta} - Bu^{(e)} - P\right)\right\} d\eta = 0 \tag{25}$$

Neglecting the first term in equation (25), one gets:

$$\int_{\eta_j}^{\eta_k}\left\{\frac{\partial N^{(e)T}}{\partial \eta}\frac{\partial u^{(e)}}{\partial \eta} + N^{(e)T}\left(A\frac{\partial u^{(e)}}{\partial \eta} - Bu^{(e)} - P\right)\right\} d\eta = 0$$

Let $u^{(e)} = N^{(e)}\phi^{(e)}$ be the linear piecewise approximation solution over the element (e), $(\eta_j \le \eta \le \eta_k)$, where $N^{(e)} = \begin{bmatrix} N_j & N_k \end{bmatrix}$, $\phi^{(e)} = \begin{bmatrix} u_j & u_k \end{bmatrix}^T$ and $N_j = \frac{\eta_k - \eta}{\eta_k - \eta_j}$, $N_k = \frac{\eta - \eta_j}{\eta_k - \eta_j}$ are the basis functions. One obtains:

$$\int_{\eta_j}^{\eta_k}\left\{\begin{bmatrix} N_j' N_j' & N_j' N_k' \\ N_j' N_k' & N_k' N_k' \end{bmatrix}\begin{bmatrix} u_j \\ u_k \end{bmatrix}\right\} d\eta + A\int_{\eta_j}^{\eta_k}\left\{\begin{bmatrix} N_j N_j' & N_j N_k' \\ N_j' N_k & N_k' N_k \end{bmatrix}\begin{bmatrix} u_j \\ u_k \end{bmatrix}\right\} d\eta - B\int_{\eta_j}^{\eta_k}\left\{\begin{bmatrix} N_j N_j & N_j N_k \\ N_j N_k & N_k N_k \end{bmatrix}\begin{bmatrix} u_j \\ u_k \end{bmatrix}\right\} d\eta = P\int_{\eta_j}^{\eta_k}\begin{bmatrix} N_j \\ N_k \end{bmatrix} d\eta$$

Where prime denotes differentiation w.r.t $'\eta'$

Simplifying we get

$$\frac{1}{l^{(e)^2}}\begin{bmatrix} 1 & -1 \\ -1 & 1 \end{bmatrix}\begin{bmatrix} u_j \\ u_k \end{bmatrix} + \frac{A}{2l^{(e)}}\begin{bmatrix} -1 & 1 \\ -1 & 1 \end{bmatrix}\begin{bmatrix} u_j \\ u_k \end{bmatrix} - \frac{B}{6}\begin{bmatrix} 2 & 1 \\ 1 & 2 \end{bmatrix}\begin{bmatrix} u_j \\ u_k \end{bmatrix} = \frac{P}{2}\begin{bmatrix} 1 \\ 1 \end{bmatrix}$$

Where $l^{(e)} = \eta_k - \eta_j = h$

Assembling the element equations for two consecutive elements $(\eta_{i-1} \le \eta \le \eta_i)$ and $(\eta_i \le \eta \le \eta_{i+1})$ following is obtained:

$$\frac{1}{l^{(e)^2}}\begin{bmatrix} 1 & -1 & 0 \\ -1 & 2 & -1 \\ 0 & -1 & 1 \end{bmatrix}\begin{bmatrix} u_{i-1} \\ u_i \\ u_{i+1} \end{bmatrix} + \frac{A}{2l^{(e)}}\begin{bmatrix} -1 & 1 & 0 \\ -1 & 0 & 1 \\ 0 & -1 & 1 \end{bmatrix}\begin{bmatrix} u_{i-1} \\ u_i \\ u_{i+1} \end{bmatrix} - \frac{B}{6}\begin{bmatrix} 2 & 1 & 0 \\ 1 & 4 & 1 \\ 0 & 1 & 2 \end{bmatrix}\begin{bmatrix} u_{i-1} \\ u_i \\ u_{i+1} \end{bmatrix} = \frac{P}{2}\begin{bmatrix} 1 \\ 2 \\ 1 \end{bmatrix} \tag{26}$$

Now put row corresponding to the node 'i' to zero, from equation (26) the difference schemes with $l^{(e)} = h$ is:

$$\frac{1}{h^2}\left[-u_{i-1} + 2u_i - u_{i+1}\right] + \frac{A}{2h}\left[-u_{i-1} + u_{i+1}\right] - \frac{B}{6}\left[u_{i-1} + 4u_i + u_{i+1}\right] = P \tag{27}$$

Simplifying the above equation (27), then we get

$$A_1 u_{i-1} + A_2 u_i + A_3 u_{i+1} = P^* \tag{28}$$

Now from equations (18), (19) and (20), following equations are obtained:

$$B_1 w_{i-1} + B_2 w_i + B_3 w_{i+1} = Q^* \tag{29}$$

$$C_1 \theta_{i-1} + C_2 \theta_i + C_3 \theta_{i+1} = R^* \tag{30}$$

$$D_1 C_{i-1} + D_2 C_i + D_3 C_{i+1} = 0 \tag{31}$$

Where $A_1 = 3Ah - Bh^2 - 6,\ A_2 = 12 - 4Bh^2,\ A_3 = -3Ah - Bh^2 - 6,\ B_1 = 3Ah - Bh^2 - 6,$
$B_2 = 12 - 4Bh^2,\ B_3 = -3Ah - Bh^2 - 6,\ C_1 = 3A(\mathrm{Pr})h + R(\mathrm{Pr})h^2 - 6,\ C_2 = 12 + 4R(\mathrm{Pr})h^2,$
$C_3 = -3A(\mathrm{Pr})h + R(\mathrm{Pr})h^2 - 6,\ D_1 = 3A(Sc)h + (k_r)(Sc)h^2 - 6,\ D_2 = 12 + 4(k_r)(Sc)h^2,$
$D_3 = -3A(Sc)h + (k_r)(Sc)h^2 - 6,\ P^* = -6h^2(Gr)\theta_i - 6h^2(Gc)\phi_i + 6h^2 Bmw_i,$
$Q^* = 6h^2 Bu_i,\ \ R^* = 6h^2 R(\mathrm{Pr})$;

Here h is the mesh size along $\eta -$ direction and index i refers to space. In the equations (28), (29), (30) and (31), taking $i = 1(1)n$ and using boundary conditions (15), then the following system of equations are obtained:

$$A_i X_i = B_i \quad i = 1(1)n \tag{32}$$

Where $A_i^{'}$s are matrices of order n and $X_i, B_i^{'}$s are column matrices having $n-$components. The above systems of equations have been solved by Thomas algorithm (Gauss – Seidel Iteration method) for velocity, temperature and concentration. Also, numerical solutions for these equations are obtained by $C-$programme. In order to prove the convergence and stability of finite element method, the computation is carried out for slightly changed values of h, running the same $C-$programme. Negligible change is observed in the values of $u,\ w,\ \theta\ \&\ C$ and also after each cycle of iteration the convergence checking is performed. $i.e.,\ \left|u^{n+1} - u^n\right| < 10^{-8}$ is satisfied at all points. Thus, it is concluded that, the finite element scheme is stable and convergent.

4. RESULT AND DISCUSSIONS

We solve the similarity equations (17), (18), (19) and (20) numerically by applying finite element method subject to the boundary conditions given by (15). Graphical representations of the numerical results are illustrated in figure (1) through figure (20) to show the influences of different numbers on the boundary layer flow. In this study, we investigate the influence of the effects of material parameters such as Grashof number (Gr), Modified Grashof number (Gc), Prandtl number (Pr), Schmidt number (Sc), Hartmann number (M), Hall parameter (m), Thermal radiation parameter (R) and Chemical Reaction (k_r) separately in order to clearly observe their respective effects on the velocity, temperature and concentration profiles of the flow. And also skin – friction coefficients $(\tau_1\ \&\ \tau_2)$, Rate of heat and mass transfer coefficients in terms of Nusselt number (Nu) and Sherwood number (Sh) respectively have been observed through graphically. During the course of numerical calculations of the primary velocity (u), secondary velocity (w), temperature (θ) and concentration (ϕ), the values of the Prandtl number are chosen for Mercury (Pr = 0.025), Air at 25^oC and one atmospheric pressure (Pr = 0.71), Water (Pr = 7.00) and Water at 4^oC (Pr = 11.40). To focus out attention on numerical values of the results obtained in the study the values of Schmidt number (Sc) are chosen for the gases representing diffusing chemical species of most common interest in air namely Hydrogen (Sc = 0.22), Helium (Sc = 0.30), Water – vapour (Sc = 0.60), Oxygen (Sc = 0.66) and Ammonia (Sc = 0.78). To examine the effect of parameters related to the problem on the velocity field and skin – friction numerical computations are carried out at Pr = 0.71. To find solution of this problem, we have placed an infinite vertical plate in a finite length in the flow. Hence, we solve the entire problem in a finite boundary. However, in

the graphs, the η values vary from 0 to 4, and the velocity, temperature, and concentration tend to zero as η tend to 4. This is true for any value of η. Thus, we have considered finite length.

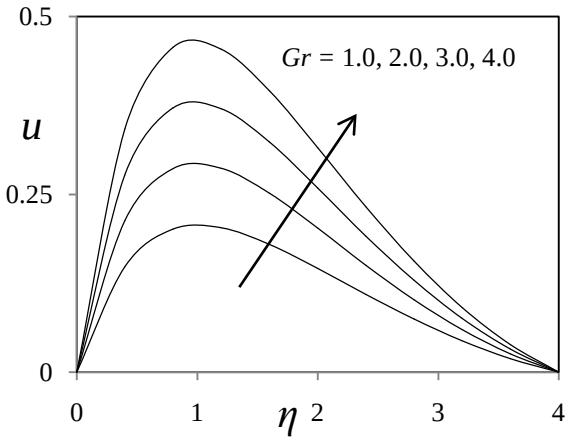

Figure 2. Effect of Grashof number on primary velocity profiles

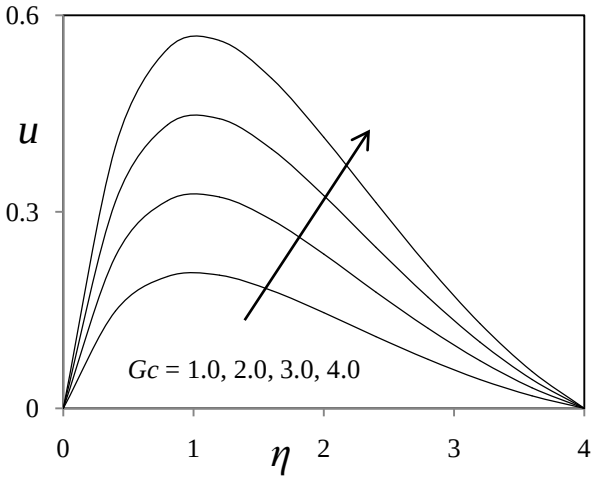

Figure 3. Effect of Modified Grashof number on primary velocity profiles

The temperature and the species concentration are coupled to the velocity via Grashof number (Gr) and Modified Grashof number (Gc) as seen in equation (17). For various values of Grashof number and Modified Grashof number, the velocity profiles u are plotted in figures (2) and (3). The Grashof number (Gr) signifies the relative effect of the thermal buoyancy force to the viscous hydrodynamic force in the boundary layer. As expected, it is observed that there is a rise in the velocity due to the enhancement of thermal buoyancy force. Also, as Gr increases, the peak values of the velocity increases rapidly near the porous plate and then decays smoothly to the free stream velocity. The Modified Grashof number (Gc) defines the ratio of the species buoyancy force to the viscous hydrodynamic force. As expected, the fluid velocity increases and the peak value is more distinctive due to increase in the species buoyancy force. The velocity distribution attains a distinctive maximum value in the vicinity of the plate and then decreases properly to approach the free stream value. It is noticed that the velocity increases with increasing values of the Modified Grashof number (Gc).

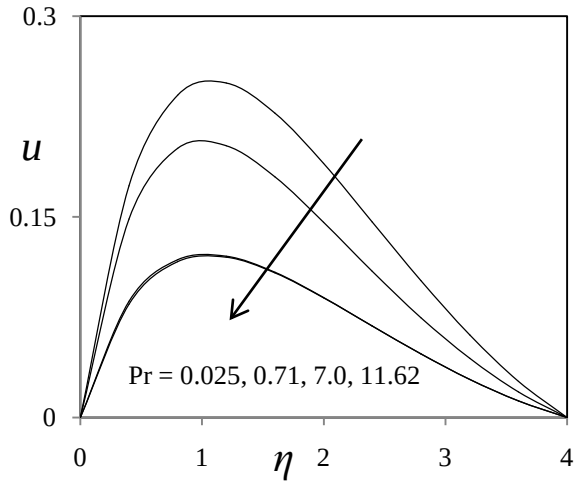

Figure 4. Effect of Prandtl number on primary velocity profiles

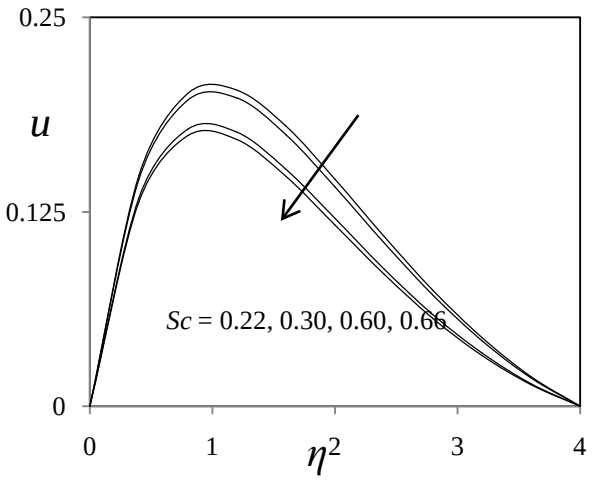

Figure 5. Effect of Schmidt number on primary velocity profiles

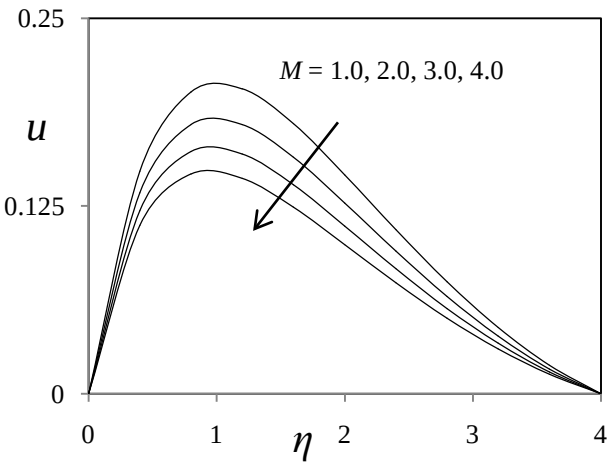

Figure 6. Effect of Hartmann number on primary velocity profiles

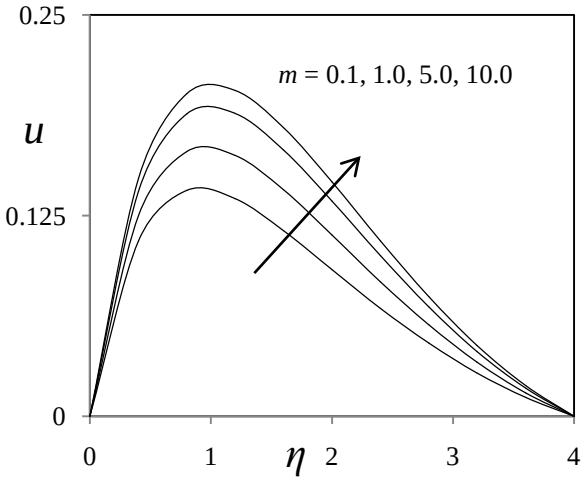

Figure 7. Effect of Hall parameter on primary velocity profiles

Figure (4) depicts the effect of Prandtl number on primary velocity profiles in presence of foreign species such as Mercury (Pr = 0.025), Air (Pr = 0.71) Water (Pr = 7.00) and Water at $4^{o}C$ (Pr = 11.40). We observe that from figure (4) the primary velocity decreases with increasing of Prandtl number (Pr). The nature of primary velocity profiles in presence of foreign species such as Hydrogen (Sc = 0.22), Helium (Sc = 0.30), Water – vapour (Sc = 0.60) and Oxygen (Sc = 0.66) are shown in figure (5). The flow field suffers a decrease in primary velocity at all points in presence of heavier diffusing species. The effect of the Hartmann number (M) is shown in figure (6). It is observed that the primary velocity of the fluid decreases with the increase of the magnetic field number values. The decrease in the primary velocity as the Hartmann number (M) increases is because the presence of a magnetic field in an electrically conducting fluid introduces a force called the Lorentz force, which acts against the flow if the magnetic field is applied in the normal direction, as in the present study. This resistive force slows down the fluid velocity component as shown in figure (6). Figure (7) depicts the primary velocity profiles as the Hall parameter (m) increases. We see that u increases as (m) increases. It can also be observed that u profiles approach their classical values when the Hall parameter (m) becomes large (m > 5).

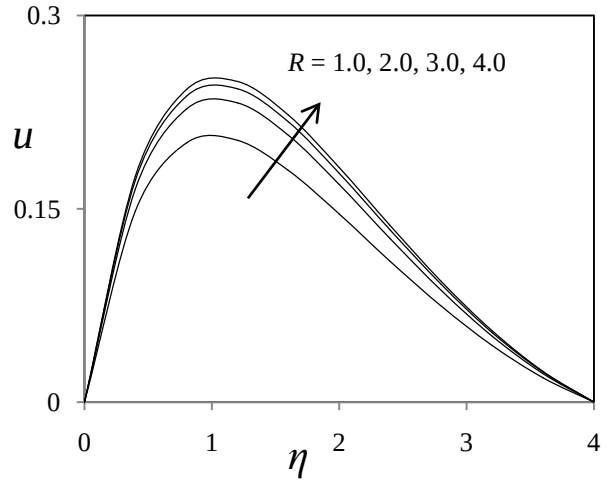

Figure 8. Effect of Effect of thermal radiation parameter on primary velocity profiles

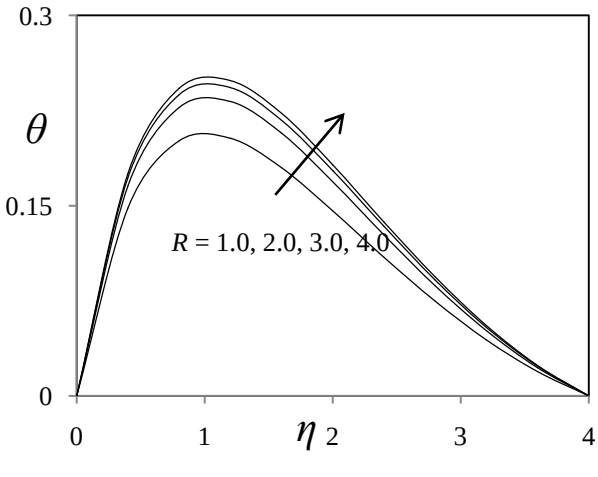

Figure 9. Effect of thermal radiation parameter on temperature profiles

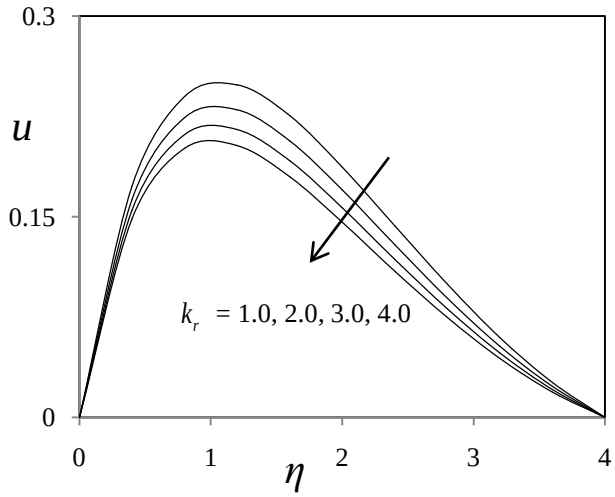

Figure 10. Effect of Chemical reaction parameter on primary velocity profiles

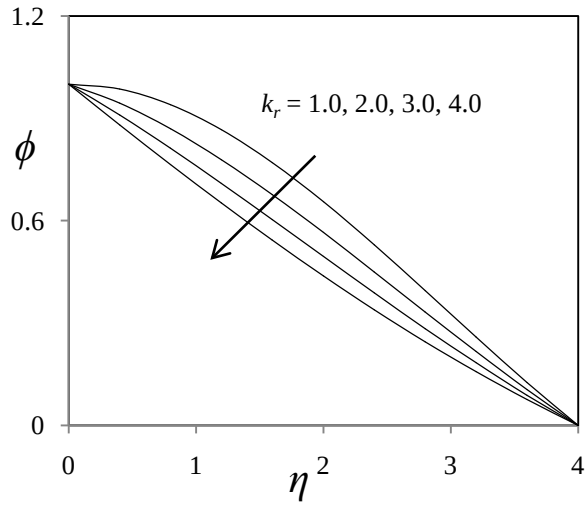

Figure 11. Effect of Chemical reaction parameter on concentration profiles

The effects of the thermal radiation parameter R on the primary velocity and temperature profiles in the boundary layer are illustrated in figures (8) and (9) respectively. Increasing the thermal radiation parameter (R) produces significant increase in the thermal condition of the fluid and its thermal boundary layer. This increase in the fluid temperature induces more flow in the boundary layer causing the velocity of the fluid there to increase. Figures (10) and (11) display the effects of the chemical reaction parameter (k_r) on the velocity and concentration profiles, respectively. As expected, the presence of the chemical reaction significantly affects the concentration profiles as well as the velocity profiles. It should be mentioned that the studied case is for a destructive chemical reaction (k_r). In fact, as chemical reaction (k_r) increases, the considerable reduction in the velocity profiles is predicted, and the presence of the peak indicates that the maximum value of the velocity occurs in the body of the fluid close to the surface but not at the surface. Also, with an increase in the chemical reaction parameter, the concentration decreases. It is evident that the increase in the chemical reaction (k_r) significantly alters the concentration boundary layer thickness but does not alter the momentum boundary layers.

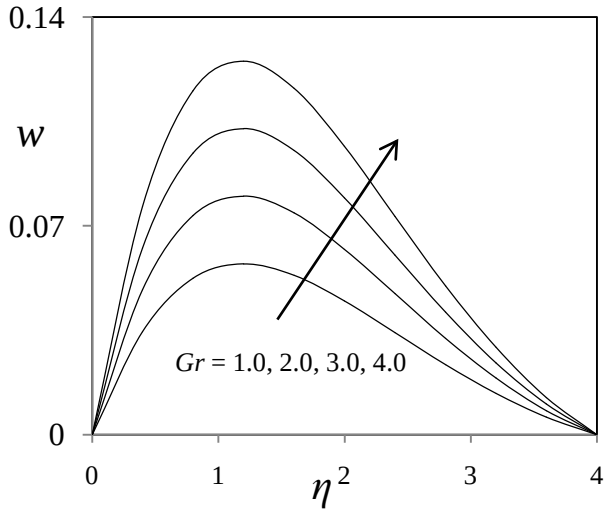

Figure 12. Effect of Grashof number on secondary velocity profiles

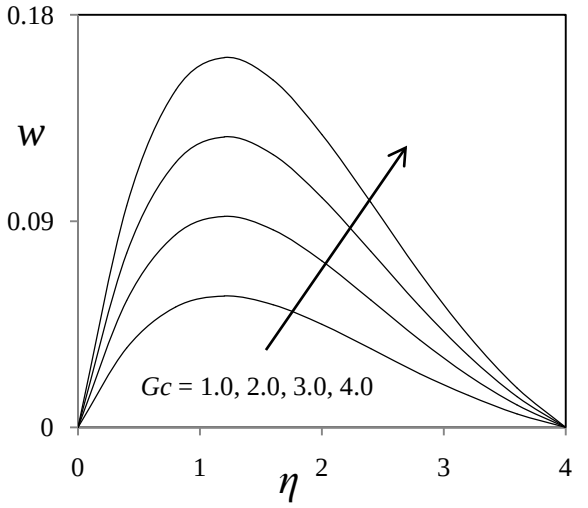

Figure 13. Effect of Modified Grashof number on secondary velocity profiles

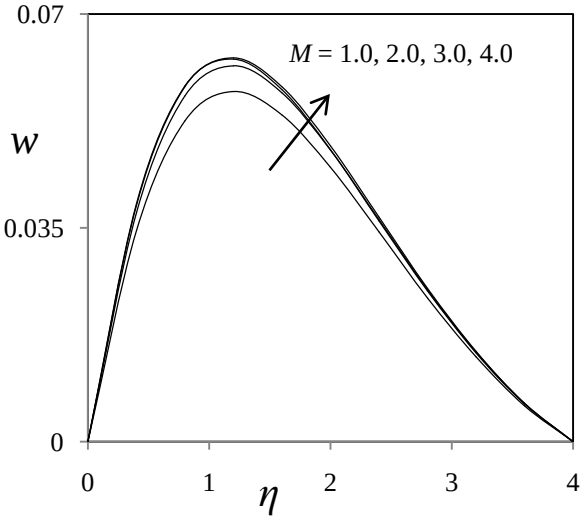

Figure 14. Effect of Hartmann number on secondary velocity profiles

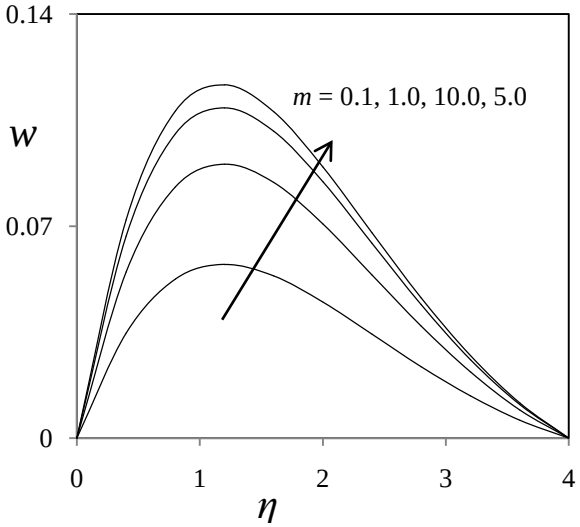

Figure 15. Effect of Hall parameter on secondary velocity profiles

In figures (12) and (13), we see the influence of the both heat and mass transfer on secondary velocity of the flow. It can be seen that as both the heat and mass transfer increases, this velocity component increases as well. In figure (14) we have the influence of the Hartmann number (M) on the secondary velocity. It can be seen that as the values of this parameter increase, the secondary velocity increases. In figure (15), we see that w profiles increase for m < 1 and decrease for m > 1. The effect of thermal radiation parameter (R) is shown in the figure (16). From this figure, we observe that the secondary velocity is increasing with increasing values of thermal radiation parameter (R). In figure (17) we have the effect of the chemical reaction parameter (k_r) on the secondary velocity. It can be seen that as the values of this parameter increases, the secondary velocity also increases.

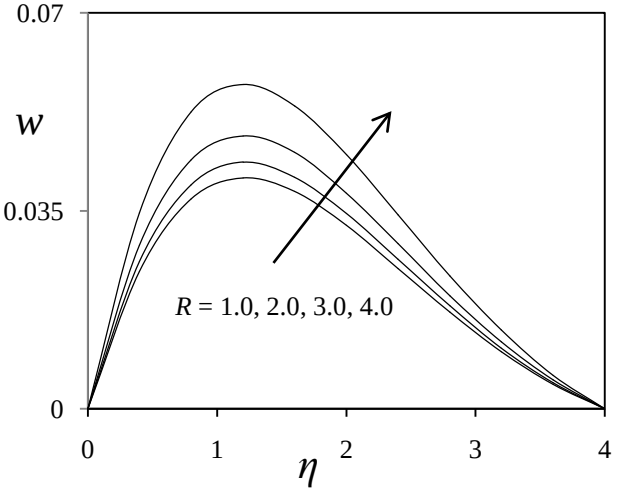

Figure 16. Effect of thermal radiation parameter on secondary velocity profiles

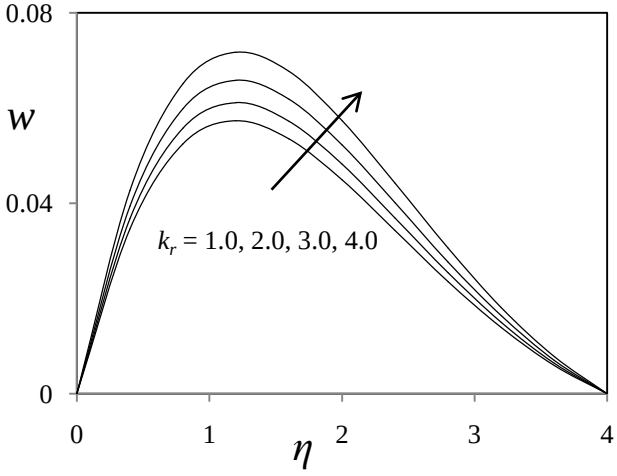

Figure 17. Effect of Chemical reaction parameter on secondary velocity profiles

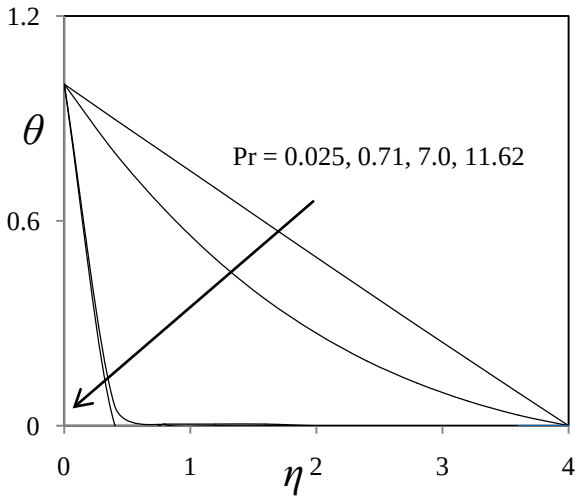

Figure 18. Effect of Prandtl number on temperature profiles

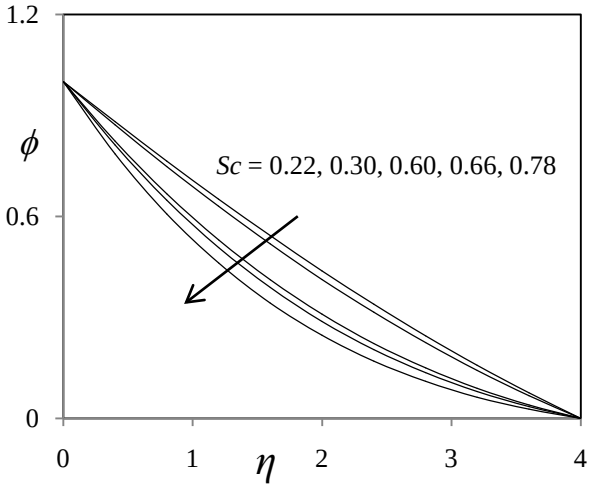

Figure 19. Effect of Schmidt number on concentration profiles

In figure (18) we depict the effect of Prandtl number $(\Pr)$ on the temperature field. It is observed that an increase in the Prandtl number leads to decrease in the temperature field. Also, temperature field falls more rapidly for water in comparison to air and the temperature curve is exactly linear for mercury, which is more sensible towards change in temperature. From this observation it is conclude that mercury is most effective for maintaining temperature differences and can be used efficiently in the laboratory. Air can replace mercury, the effectiveness of maintaining temperature changes are much less than mercury. However, air can be better and cheap replacement for industrial purpose. This is because, either increase of kinematic viscosity or decrease of thermal conductivity leads to increase in the value of Prandtl number $(\Pr)$. Hence temperature decreases with increasing of Prandtl number $(\Pr)$. Figure (19) shows the concentration field due to variation in Schmidt number (Sc) for the gasses Hydrogen, Helium, Water – vapour, Oxygen and Ammonia. It is observed that concentration field is steadily for Hydrogen and falls rapidly for Oxygen and Ammonia in comparison to Water – vapour. Thus Hydrogen can be used for maintaining effective concentration field and Water – vapour can be used for maintaining normal concentration field.

Table – 1: Shear stress $(\tau_1 \ \& \ \tau_2)$ results

Gr	Gc	Sc	Pr	M	m	R	k_r	τ_1	τ_2
1.0	1.0	0.22	0.71	1.0	1.0	1.0	1.0	3.05145184	0.54742265
2.0	1.0	0.22	0.71	1.0	1.0	1.0	1.0	3.91520651	0.76560154
1.0	2.0	0.22	0.71	1.0	1.0	1.0	1.0	4.23890987	0.87657820
1.0	1.0	0.30	0.71	1.0	1.0	1.0	1.0	3.00553394	0.53103614
1.0	1.0	0.22	7.00	1.0	1.0	1.0	1.0	2.20466682	0.33250178
1.0	1.0	0.22	0.71	2.0	1.0	1.0	1.0	2.82361172	0.58933395
1.0	1.0	0.22	0.71	1.0	2.0	1.0	1.0	3.11262957	0.86450258
1.0	1.0	0.22	0.71	1.0	1.0	2.0	1.0	3.32723640	0.55904015
1.0	1.0	0.22	0.71	1.0	1.0	1.0	2.0	2.86541824	0.58243026

The profiles for shear stress (τ_1) due to primary velocity under the effects of Grashof number, Modified Grashof number, Schmidt number, Prandtl number, Hartmann number, Hall parameter, Chemical reaction and Radiation parameter are presented in table – 1. We observe from the above table – 1, the shear stress (τ_1) rises under the effects of Grashof number, Modified Grashof number, Hall parameter, Radiation parameter and falls under the effects of Schmidt number, Prandtl number, Chemical reaction and Hartmann number. The profiles for shear stress (τ_2) due to secondary velocity under the effects of Grashof number, Modified Grashof number, Schmidt number, Prandtl number, Hartmann number, Hall parameter, Chemical reaction and Thermal radiation parameter are presented in the table – 1. We see from the above table – 1 the shear stress (τ_2) due to secondary velocity increases under the effects Grashof number, Modified Grashof number, Hartmann number, Hall parameter and Radiation parameter. Also, the shear stress (τ_2) decreases under the effects of Schmidt number, Chemical reaction and Prandtl number. The profiles for Nusselt number (Nu) due to temperature profiles under the effect of Prandtl number and Radiation parameter are presented in table – 2. We see from this table the Nusselt number rises under the effect of Thermal radiation parameter and falls

under the effect of Prandtl number. The profiles for Sherwood number (Sh) due to concentration profiles under the effect of Schmidt number and Chemical reaction is presented in the table – 2. We see from this table – 2 the Sherwood number decreases under the effects of Schmidt number and Chemical reaction.

Table – 2: Rate of heat and mass transfer (Nu & Sh) values

Pr	R	Nu	Sc	k_r	Sh
0.71	1.0	5.93616187	0.22	1.0	7.36074871
7.00	1.0	4.01793047	0.30	1.0	7.28005841
0.71	2.0	6.15979984	0.22	2.0	7.16883068

Table – 3: τ_1 is the Shear stress results obtained in the present study, and τ_1^* is the Shear stress results obtained by Seddeek and Aboeldahab [22].

Gr	Pr	M	m	R	τ_1	τ_1^*
1.0	0.71	1.0	1.0	1.0	2.5544	2.5518
2.0	0.71	1.0	1.0	1.0	3.3879	3.3854
1.0	7.00	1.0	1.0	1.0	2.2473	2.2457
1.0	0.71	2.0	1.0	1.0	2.1148	2.1126
1.0	0.71	1.0	2.0	1.0	2.6481	2.6460
1.0	0.71	1.0	1.0	2.0	2.6642	2.6629

In order to ascertain the accuracy of the numerical results, the present results are compared with the previous analytical results in absence of chemical reaction of Mohammed Seddeek and Aboeldahab [22] for Gr = 1.0, $\Pr$ = 0.71, M = 1.0, m = 1.0 and R = 1.0 in table – 3. They are found to be in an excellent agreement.

5. CONCLUSIONS

This work investigated the effect of chemical reaction on an unsteady magnetohydrodynamic free convection flow near a vertical porous plate immersed in a porous medium with hall current and thermal radiation. The similarity solutions were obtained using suitable transformations and the resulting similarity ordinary differential equations were solved by using finite element method. A parametric study illustrating the influence of different flow parameters on velocity, temperature and concentration fields are investigated. The shearing stress at the plate due to primary and secondary velocity fields and rate of heat and mass transfer due to temperature and concentration respectively are obtained in non – dimensional form. The results are presented graphically and in tabular form. We conclude that the flow field and the quantities of physical interest are significantly influenced by these numbers.

1. The primary velocity increases as the Grashof number, Modified Grashof number, Hall parameter and Thermal radiation parameter increases. However, the primary velocity was found to decreases as the Schmidt number, Prandtl number, Hartmann number and Chemical reaction parameter.
2. The secondary velocity increases as the Grashof number, Modified Grashof number, Hartmann number, Hall parameter and Thermal radiation parameter increases. However, the secondary velocity was found to decreases as the Chemical reaction increases.
3. The fluid temperature was found to increases as the Thermal radiation parameter and decreases as the Prandtl number increases.
4. The concentration decreases as the Schmidt number and Chemical reaction parameter increases.
5. The Nusselt number due to temperature profile rises under the effect of Thermal radiation parameter and falls under the effect of Prandtl number.
6. The Sherwood number due to concentration profile decreases under the effect of Schmidt number and Chemical reaction parameter.
7. On comparing the skin – friction results with the results of Mohammed Seddeek and Aboeldahab [22] it can be seen that they agree very well.

REFERENCES

[1] Anand Rao, J., Srinivasa Raju, R. and Shivaiah, S., (2012). Chemical reaction effects on an unsteady MHD free convection fluid flow past a semi – infinite vertical plate embedded in a porous medium with Heat Absorption, *Journal of Applied Fluid Mechanics*, Vol. 5, No. 3, pp. 63 – 70.

[2] Anand Rao, J., Srinivasa Raju, R. and Shivaiah, S., (2012). Finite element solution of heat and mass transfer in MHD flow of a viscous fluid past a vertical plate under oscillatory suction velocity, *Journal of Applied Fluid Mechanics*, Vol. 5, No. 3, pp. 1 – 10.

[3] Anand Rao, J., Srinivasa Raju, R. and Shivaiah, S., (2012). Finite element solution of MHD transient flow past an impulsively started infinite horizontal porous plate in a rotating fluid with Hall Current, *Journal of Applied Fluid Mechanics*, Vol. 5, No. 3, pp. 105 – 112.

[4] Bala Anki Reddy, P. and Bhaskar Reddy, N., (2010). Radiation effects on MHD combined convection and mass transfer flow past a vertical porous plate embedded in a porous medium with heat generation, *Int. J. of Appl. Math. and Mech.*, Vol. 6, No. 18, pp. 33 – 49.

[5] Baoku, I. G., Israel – Cookey, C. and Olajuwon, B. I., (2012). Influence of thermal radiation on a transient MHD Couette flow through a porous medium, *Journal of Applied Fluid Mechanics*, Vol. 5, No. 1, pp. 81 – 87.

[6] Chamkha, A. J. and Ahmed, S. E., (2011). Similarity solution for unsteady MHD flow near a stagnation point of a three – dimensional porous body with heat and mass transfer, Heat Generation/Absorption and Chemical Reaction, *Journal of Applied Fluid Mechanics*, Vol. 4, No. 2, Issue 1, pp. 87 – 94.

[7] Cogley, A. C., Vincenti, W. G. and Gilles, S. E., (1968). Differential Approximation for Radiative Transfer in a non – gray gas near equilibrium, *AIAAJ*, Vol. 6, pp. 551 – 556.

[8] Gnaneswara Reddy, M. and Bhaskar Reddy, N., (2010). Radiation and mass transfer effects on unsteady MHD free convection flow past a vertical porous plate with viscous dissipation, *Int. J. of Appl. Math. and Mech.*, Vol. 6, No. 6, pp. 96 – 110.

[9] Greif, R., Habib, I. S. and Lin, J. C., (1970). Laminar convection of a radiating gas in a vertical channel, *Journal of Fluid Mechanics*, Vol. 46, pp. 513 – 520.

[10] Kesavaiah, D. Ch., Satyanarayana, P. V. and Venkataramana, S., (2011). Effects of the chemical reaction and radiation absorption on an unsteady MHD convective heat and mass transfer flow past a semi – infinite vertical permeable moving plate embedded in a porous medium with heat source and suction, *Int. J. of Appl. Math. and Mech.*, Vol. 7, No. 1, pp. 52 – 69.

[11] Kishore, P. M., Rajesh, V. and Varma, S. V. K., (2010).The effects of thermal radiation and viscous dissipation on MHD heat and mass diffusion flow past a surface embedded in a porous medium, *Int. J. of Appl. Math. and Mech.*, Vol. 6, No. 11, pp. 79 – 97.

[12] Loganathan, P., Kulandaivel, T. and Muthucumaraswamy, R., (2008). First order chemical reaction on moving semi – infinite vertical plate in the presence of optically thin gray gas, *Int. J. of Appl. Math. and Mech.*, Vol. 4, No. 5, pp. 26 – 41.

[13] Mansour, M. A., El – Anssary, N. F. and Aly, A. M., (2008). Effect of chemical reaction and viscous dissipation on MHD natural convection flows saturated in porous media with suction or injection, *Int. J. of Appl. Math. and Mech.*, Vol. 4, No. 2, pp. 60 – 76.

[14] Mohammed Ibrahim, S. and Bhaskar Reddy, N., (2012). Radiation and mass transfer effects on MHD free convection flow along a stretching surface with viscous dissipation and heat generation, *Int. J. of Appl. Math. and Mech.*, Vol. 8, No. 8, pp. 1 – 21.

[15] Prasad, V. R., Muthucumaraswamy, R. and Vasu, B., (2010). Radiation and mass transfer effects on unsteady MHD free convection flow past a vertical porous plate embedded in a porous medium: a numerical study. *Int. J. of Appl. Math. and Mech.*, 6, 19, pp. 1 – 21.

[16] Rajesh, V. and Varma, S. V. K., (2010). Heat source effects on MHD flow past an exponentially accelerated vertical plate with variable temperature through a porous medium, *Int. J. of Appl. Math. and Mech.*, Vol. 6, No. 12, pp. 68 – 78.

[17] Raji Reddy, S. and Srihari, K., (2009). Numerical solution of unsteady flow of a radiating and chemically reacting fluid with time – dependent suction, *Indian Journal of Pure and Applied physics*, Vol. 47, pp. 7 – 11.

[18] Sankar Reddy, T., Ramachandra Prasad, V., Roja, P. and Bhaskar Reddy, N., (2010). Radiation effects on MHD mixed convection flow of a micropolar fluid past a semi – infinite vertical plate in a porous medium with heat absorption, *Int. J. of Appl. Math. and Mech.*, Vol. 6, No. 18, pp. 80 – 101.

[19] Schlichting, H., (1968). *Boundary Layer Theory*, McGraw – Hill, New York.

[20] Seth, G. S., Nandkeolyar, R. and Ansari, Md. S., (2012). Effects of Hall current and rotation on unsteady MHD Couette flow in the presence of an inclined magnetic field, *Journal of Applied Fluid Mechanics*, Vol. 5, No. 2, pp. 67 – 74.

[21] Vasu, B., Ramachandra Prasad, V. and Bhaskar Reddy, N., (2011). Radiation and mass transfer effects on transient free convection flow of a dissipative fluid past semi – infinite vertical plate with uniform heat and mass flux, *Journal of Applied Fluid Mechanics*, Vol. 4, No. 1, pp. 15 – 26.

[22] Mohamed, A., Seedeek and Emad M. Aboeldahab, (2001). Radiation effects on unsteady MHD free convection with hall current near an infinite vertical porous plate, *IJMMS*, Vol. 26, No. 4, pp. 249 – 255.

Source of support: Nil, Conflict of interest: None Declared